SIMULATION OF SELF-PRESSURIZATION IN CRYOGENIC PROPELLANT TANK

Liang Chen*[1] Bangcheng Ai[1] Siyuan Chen[1] Guozhu Liang[2]
*Author for correspondence
[1]China Academy of Aerospace Aerodynamics,
Beijing 100074,
[2] School of Astronautics, Beihang University,
Beijing 100191,
China,
*E-mail: chenliang15@buaa.edu.cn

ABSTRACT

In order to predict the pressure and investigate the interrelation among the physical processes in cryogenic propellant tanks, a 2D axial symmetry Volume-of-Fluid (VOF) computational fluid dynamic (CFD) model including a liquid propellant phase and a mixture real gas phase is established. The propellant phase change model is based on the assumption of thermodynamic equilibrium. Two comparisons between the simulation results and the self-pressurization tests of two different liquid hydrogen tanks are made to validate the model. And the deviations of pressure in the tanks are 2.7%~6.1%. The results indicate that the evaporation induced by the initial overheat is the key factor of the pressure rising in the liquid hydrogen tank at the beginning of self-pressurization, but has less influence when the tank becomes saturated.

INTRODUCTION

Heat leaks may cause thermal stratification and pressure rise in the cryogenic tanks when a rocket is parking at the launch site after propellant loaded. If the standby state were too long, flammable propellant vapor would be vented to release the pressure. So prediction of pressure rise in the cryogenic propellant tank is important for the safety of launch vehicles.

There are two main methods including lumped and CFD methods adopted in existing research works. Lumped models are widely used in pressure prediction of launch vehicle tanks but not able to reflect the details of physical processes. Van Dresar et al. [1] founded that thermodynamics under-predicted the self-pressurization rate. The effect of fill level on the pressurization rate was difficult to discern from the experimental data in a liquid hydrogen tank test implemented by NASA[2, 3]. The zonal method is an improved method where the liquid vapor system is divided into zones at constant temperatures. Estey et al.[4]added a separated zone bounding the interface in a model with another two separated zones representing the two phases. Schallhorn et al.[5]partitioned the liquid into annular boundary layer zones and axial zones in the bulk. The results of these models depend on the correlations which are used to model heat and mass transport between the different zones. However, spatial distribution of many variables such as temperature, velocity, and pressure are not able to be obtained through lumped methods.

Thus several investigators have tried to use CFD models instead of zonal ones. Barsi et al.[6] established a self-pressurization model where the cryogenic tank was modeled as an incompressible-incompressible system considering phase change. Gas compressibility, as well as heat and mass exchange on interface, were modeled in a lumped fashion, and then coupled to the bulk transport equations. The predicted ullage pressure history agreed well with the low fill levels test[2, 3]. But the deviation of pressure in the high fill levels of 83% test was 37%. Mattick et al.[7]got a better simulation on that test using CRUNCH CFD, and the deviation is 15%~20%.Mukka and Rahman[8] conducted a steady-state finite element analysis of a liquid jet entering a tank including both the liquid and vapor phases, but their results were thought to be unreliable. The accuracy and validity of these models depend on the fidelity of using global mass and energy balances at the interface to account for phase change. The accuracy and validity of these simplified models are not so satisfying. Moreover, a lumped vapor model cannot interpret the gas convection and the heat transfer between the gas region and the bounding wall, so they are not suitable for studying various interacting mechanisms.

In order to obtain better depiction of physical processes, a CFD model with a compressible gas phase and a liquid propellant phase using volume of fluid (VOF) method is established. The gas phase is modeled using real gas model and mixed gas diffusion model. The phase change model is built on the assumption of thermodynamic equilibrium.

NOMENCLATURE

ρ	[kg/m^3]	Fluid density
p	[Pa]	Pressure
E	[J]	Energy
T	[K]	Temperature
k	[W/(m·K)]	Thermal conductivity
α	[-]	Volume fraction
Y	[-]	Specie mass fraction
c_p	[J/kg]	Specific heat
R	[J/(mol·K)]	Gas constant
M	[kg/mol]	Molar mass
h	[J/kg]	Enthalpy or heat

$\vec{v}$	[m/s]	Velocity vector
$\vec{g}$	[m/s^2]	Gravity acceleration vector
$\dot{m}$	[kg/(m^3·s)]	Mass exchange rate density between the gas and liquid phase
$\dot{Q}$	[W/(m^3·s)]	Volumetric heat generation density induced by mass transfer between the gas and liquid phases
S	[1/(m^3·s)]	Species change rate density.

Special characters

$\bar{\bar{\tau}}$	[Pa]	Stress tensor

Subscripts

eff	Volumetric effective expression
i	Gas component number
L	Latent heat
q	Phase number
l	Liquid
g	Gas
V	Propellant vapor
sat	Saturation

CRYOGENIC TANK

The typical cryogenic tank is illustrated in Fig. 1. The liquid phase is liquid hydrogen or oxygen. And the gas phase is the vapor or mixture of the propellant vapor and the pressurized gas. The CFD model is considered with gas convection, heat transfer in the wall area, vaporization or condensation on the gas-liquid interface and the area near the tank inner walls.

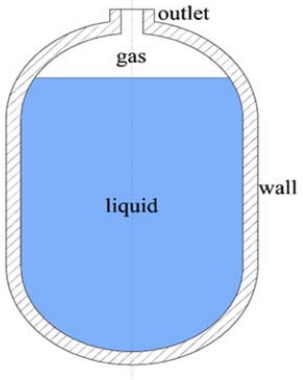

Fig. 1 Schematic of a cryogenic tank

This paper considers a liquid hydrogen tank self-pressurization test conducted by a Chinese research institute. The LH2 test tank with the diameter of about 3m is exposed to the surrounding environment. And the heat transfer between them is forced convection affected by ambient temperature and wind speed. The tank wall contains an inner aluminum alloy layer and an outer heat insulation layer attached on aluminum.

MATHEMATICAL MODEL

Control Equations

The governing equations used for describing flow and heat transfer in the tank are given as follows:

Continuity equation:

$$\frac{\partial \rho}{\partial t}+\nabla\cdot\left(\rho\vec{v}\right)=\dot{m} \qquad (1)$$

Momentum equation:

$$\frac{\partial}{\partial t}\left(\rho\vec{v}\right)+\nabla\cdot\left(\rho\vec{v}\vec{v}\right)=-\nabla p+\nabla\cdot\bar{\bar{\tau}}+\rho\vec{g} \qquad (2)$$

Energy equation:

$$\frac{\partial}{\partial t}\left(\rho E\right)+\nabla\cdot\left(\vec{v}\left(\rho E+p\right)\right)=\nabla\cdot\left(k_{\text{eff}}\nabla T+\left(\bar{\bar{\tau}}_{\text{eff}}\cdot\vec{v}\right)\right)+\dot{Q} \qquad (3)$$

The momentum change caused by phase change is neglected. Volume of Fluid (VOF) model which is able to track surface moment is chosen as the multi-phase model. The volume fraction equation can be written as follow:

$$\frac{1}{\rho_q}\left[\frac{\partial}{\partial t}\left(\alpha_q\rho_q\right)+\nabla\cdot\left(\alpha_q\rho_q\vec{v}_q\right)\right]=\frac{\dot{m}_q}{\rho_q} \qquad (4)$$

Phase Change Model

Cryogen vaporization is one of the main causes of mass loss and self-pressurization in storage tanks [9]. The bulk liquid in propellant tanks is saturated or sub-cooled initially after precooling, or turns to be sub-cooled after pressurization. So it is reasonable to assume that phase change only occurs at the heating wall surface and the gas-liquid interface including the bubbles surfaces and the liquid bulk's free surface.

Vaporization may take place in near wall layer due to net heat leaking into the tank from surrounding environment. Assuming that the liquid adjacent to the wall is in thermodynamic equilibrium state, the liquid temperature T_{l} would be equal to saturation temperature T_{sat}. The mass and energy transfer rate per unit volume are obtained following the laws of conservation of energy when the liquid temperature exceeds the saturated value.

$$\dot{m}_{\text{v,wall}}=\frac{\rho_{\text{l}}\alpha_{\text{l}}c_{p\text{l}}\left(T_{\text{l}}-T_{\text{sat}}\right)}{h_{\text{L}}\Delta t} \qquad (5)$$

$$\dot{Q}_{\text{v,wall}}=\dot{m}_{\text{v,wall}}h_{\text{L}} \qquad (6)$$

Where Δt is the time step.

If the liquid at the interface is in thermodynamic equilibrium with the adjacent vapor, the interfacial liquid pressure p_{l} and temperature T_{l} will be equal to the value of adjacent vapor p_{g} and T_{g} according to thermal and force equilibrium without considering tension. Additionally, according to phase equilibrium, the partial pressure of the vapor $p_{i\text{g}}$ will be equal to the saturation pressure p_{sat} [10]. When $p_{i\text{g}}$ is greater than p_{sat}, vapor will condense and the mass and energy transfer rate per unit volume on the interfacial surface are shown below [11, 12]

$$\dot{m}_{\text{c,interface}}=\frac{\left(p_{i\text{g}}-p_{\text{sat}}\right)\alpha_{i\text{g}}M_i}{T_{\text{l}}R\Delta t} \qquad (7)$$

$$\dot{Q}_{\text{c,interface}}=\dot{m}_{\text{c,interface}}h_{\text{L}} \qquad (8)$$

Evaporation will occur when $p_{i\text{g}}$ is lower than p_{sat}. And the mass and energy transfer rate per unit volume are thus

$$\dot{m}_{\text{v,interface}}=\frac{\left(p_{\text{sat}}-p_{i\text{g}}\right)\alpha_{i\text{g}}M_i}{T_{\text{l}}R\Delta t} \qquad (9)$$

$$\dot{Q}_{\text{v,interface}}=\dot{m}_{\text{v,interface}}h_{\text{L}} \qquad (10)$$

Where $\dot{m}$ in eqn.(1) is given by $\dot{m}_c$ or $\dot{m}_v$, and $\dot{Q}$ in eqn.(3) is given by $\dot{Q}_c$ or $\dot{Q}_v$.

Solid Wall Heat Transfer Model

In order to obtain the accurate heat leak through the tank wall, the temperature field of the solid wall and the thermal conduction in the solid area are needed to be considered. Then the energy transfer equation is expressed as

$$\frac{\partial}{\partial t}(\rho_w h_w) = \nabla \cdot (k_w \nabla T_w) \qquad (11)$$

Where ρ_w, h_w, k_w and T_w are the density, enthalpy, thermal conductivity and temperature of the solid wall respectively.

Mixed Gas Diffusion Model

The gas in the tank could be mixture of the propellant vapor and the He as the pressurized gas. The species mass-conservation equation of the vapor is thus

$$\frac{\partial}{\partial t}(\rho Y_v) + \nabla \cdot (\rho \vec{v} Y_v) = -\nabla \cdot \vec{J}_v + S_v \qquad (12)$$

Where S_v is induced by phase change. And $\vec{J}_v$ is the vector of the vapor diffusion which is defined as

$$\vec{J}_v = -\left(\rho D_{v,m} + \frac{\mu_t}{Sc_t}\right) Y_v - D_{T,v} \frac{\nabla T}{T} \qquad (13)$$

Where $D_{v,m}$, $D_{T,v}$ and Sc_t are the mass diffuse coefficient, the thermal diffusion coefficient the Schmid number respectively.

Real Gas Model

As the cryogenic gas do not follow the perfect gas law, the Virial gas model is adopted as follow

$$Z = \frac{p_{ig}}{\rho_{ig} R T_g} \qquad (14)$$

Where Z is a polynomial of compression ratio obtained through fitting experimental data which is

$$Z = A + B\frac{p}{T} + CT + DT^2 + E\frac{p}{T^2} + F\frac{p}{T^3} + Gp^3 + \frac{H}{T} \qquad (15)$$

SIMULATION METHOD

The simulation model is established using the commercial code Fluent. A 2D axial symmetry grid including the solid region and the fluid region is selected as a suitable compromise between accuracy and computational efficiency. The interior wall of the tank is set as coupled thermal boundary to solve the heat transfer between the solid wall and the fluid. The RNG k-ε turbulence model suitable for low-Reynolds flow is applied with enhanced wall treatment. Material parameters, boundary conditions and the phase change model were coded and implemented via user-defined functions (UDF). The solution is obtained through the pressure based solver. And the discretization of equations is achieved by adopting the body-force-weighted method for pressure, the geo-reconstruct method for volume fraction and second-order upwind method for other equations. The PISO (Pressure-Implicit with Splitting of Operators) algorithm is used to couple the pressure and velocity fields.

Validation of Numerical Models

Comparison between the simulation results and a LH2 tank self-pressurization test implemented by NASA Glenn Research Center was made to validate the model. The self-pressurization experiments were performed with a 4.95 m^3 partially full LH2 tank enclosed by a vacuum chamber in early 1990s[3]. The initial condition of the tank is almost saturated after a long time boil off, in which the initial temperature, pressure and fill levels is 20.4K, 0.103MPa and 83%. The average heat flux on the tank wall is determined to be 3.5 W/m^2 computed from measured boil-off rates. The structured mesh of the LH2 tank is shown in Fig. 2. More elements are concentrated near the free surface and the tank wall where the largest solution gradients are observed.

As presented in Fig. 3, the simulated pressure is very close to the test data except in the initial transient period that was not measured in the test. As the deviation at t=1800s and t=3600 is 2.7% and 1.3% respectively, the simulation precision is better than the former research that was considered to be the best simulation results of this test[7]. The simulated pressure is almost the same as the test result after 1600s.

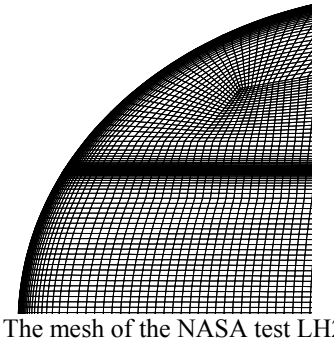

Fig. 2 The mesh of the NASA test LH2 tank

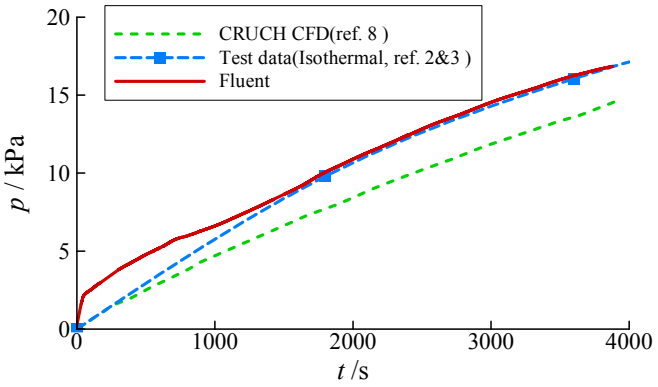

Fig. 3 Comparison between simulated result, CRUCH CFD result and test result of pressure in the NASA LH2 test tank

The simulated temperature results compared with the measured temperatures at the bottom of the tank (y=24cm) and near the gas-liquid interface (y=139cm) are illustrated in Fig. 4. It is obvious that the simulated temperature variation follows the practical trend observed in the experiment. Since the initial temperature of the case is a little higher than the boil-off tank, there is a deviation of less than 0.4% from the test data.

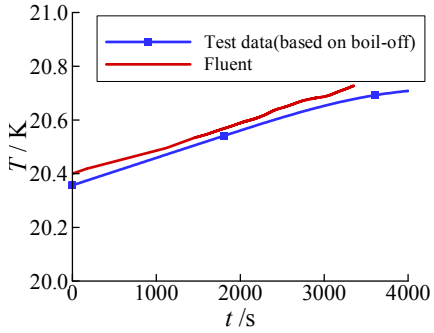

(a) y=139cm（Below the gas-liquid interface）

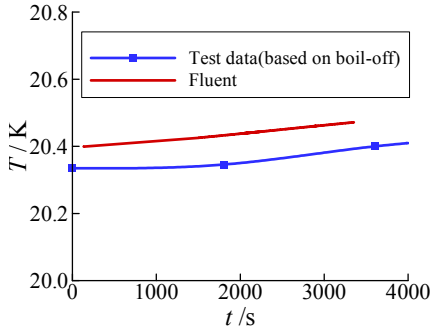

(b) y=24cm（In the liquid hydrogen ）

Fig. 4 Comparison between simulated result and test result [3] of temperature in the NASA LH2 test tank

Simulation Model of the LH2 test tank

Different form the NASA tank, the liquid hydrogen test tank was exposed to the atmosphere with nonuniform thermal boundary conditions after a boiling off stage. So the 2D thermal conduction of the solid area was considered. We select a 2D axial symmetry grid of 40041 cells shown in Fig. 5 including the meshed aluminum layer and the thermal isolating layer. Divided block meshes are required because of the large dimensional difference between the tank bulk and partial regions.

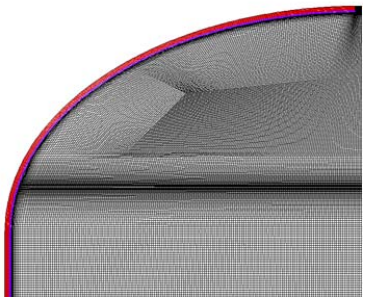

Fig. 5 The mesh of the liquid hydrogen test tank

The heat transfer coefficients are 7.345W/m^2/K around the columnar segment and 6.342W/m^2/K on the ellipsoid outer surfaces of the top head and the bottom, while the environment temperature is 288.15K, and the wind speed is 3 m/s. As there is precooling before propellant fully loaded, we set the initial thermal condition of propellant to be 20.3K, a little higher than the saturation temperature as 20.28K under the pressure of 1 atm.

RESULTS AND DISCUSSION

As shown in Fig. 6 and Fig. 7, the simulated pressure of the tank increases very fast at the beginning, then decreases to a stage of slow rise after t=50s. But the test result show a longer period of rapid increase. The initial deviation between the simulated pressure and the test result decreases with time. The average simulated pressure rise rate between t=700s and 1900s is 85.13Pa/s, which is only 6.1% less than the practical rate as 90.33Pa/s. Moreover, there is a slow growth trend in both the two pressure rise rates as reflected by Fig. 7.

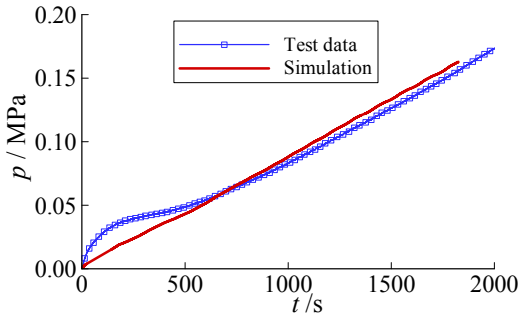

Fig. 6 Comparison of simulated result and test result of pressure in the liquid hydrogen test tank

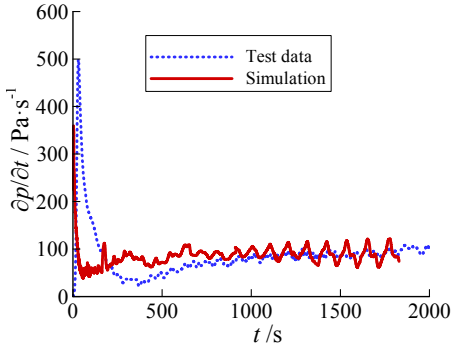

Fig. 7 Comparison of simulated result and test result of pressure rise rate in the liquid hydrogen test tank

As presented in Fig. 7 and Fig. 8, the evaporation rate and the pressure rise rate have the similar trend that rising slowly after a peak and a valley. Since the heat flux on the wall keeps decreasing, it is indicated that the vaporization is the key factor of pressure rise. And the heat leakage from inner wall surface plays a minor role in pressure rise.

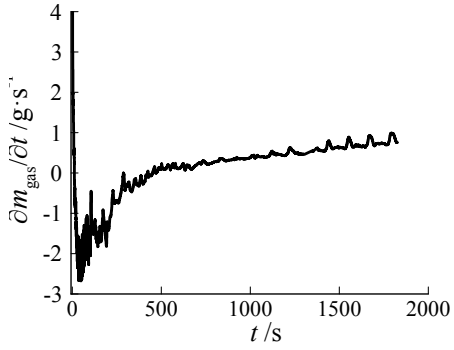

Fig. 8 Simulated result of evaporation rate in the liquid hydrogen test tank

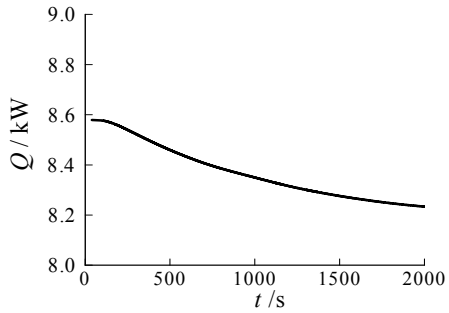

Fig. 9 Simulated result of heat flux on wall surface of the liquid hydrogen test tank

The simulated results also reveal the interrelations among phase change, convection, heat transfer and pressure variation. Fig. 10 reflects the thermal stratification of liquid hydrogen. And Fig. 11 shows convection near the gas-liquid interface. Under the heating from the wall and the mixed gas of higher temperature, the liquid temperature ascent along with altitude rising weakens convection near the free liquid surface as shown in Fig. 11. As shown in Fig. 10 and Fig. 12, the phenomenon promotes uniformity along radial direction and restrains evaporation as little heated liquid can flow to the free surface.

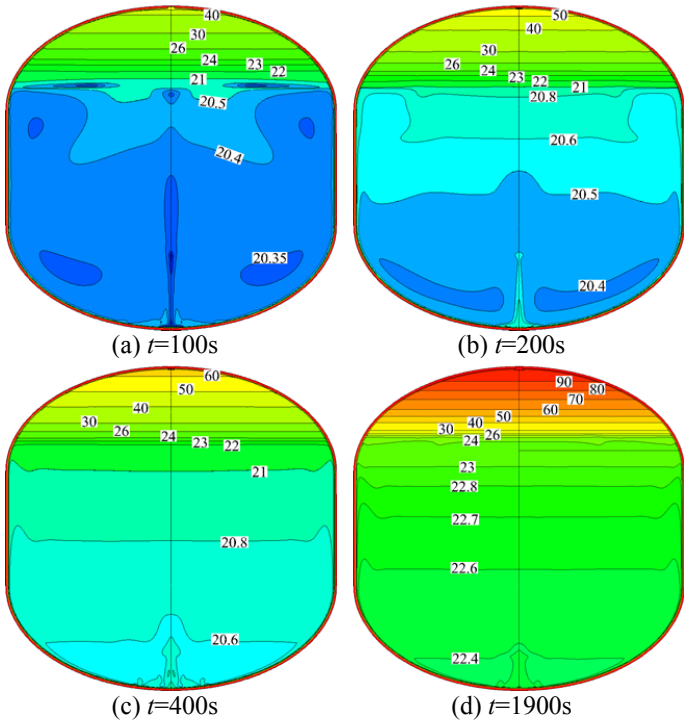

Fig. 10 Temperature of the LH2 test tank

It is inferred that the peaks of the simulated pressure and evaporation rate in the initial several seconds shown in Fig. 7 is induced by the slight overheat of the liquid hydrogen. So the rapid growth of the practical pressure may have the same cause. A simulation with initial average temperature of about 21.5K is carried out to compare with the previous result with initial average temperature of about 20.3K which is near the saturated temperature. Fig. 13 shows that the simulated pressure change trend with initially overheated condition is closer to the actual variation in the transient period of the test. Fig. 14 indicates that the initial zooming of the pressure is attributed to the significant evaporation rate as the liquid hydrogen is overheated initially.

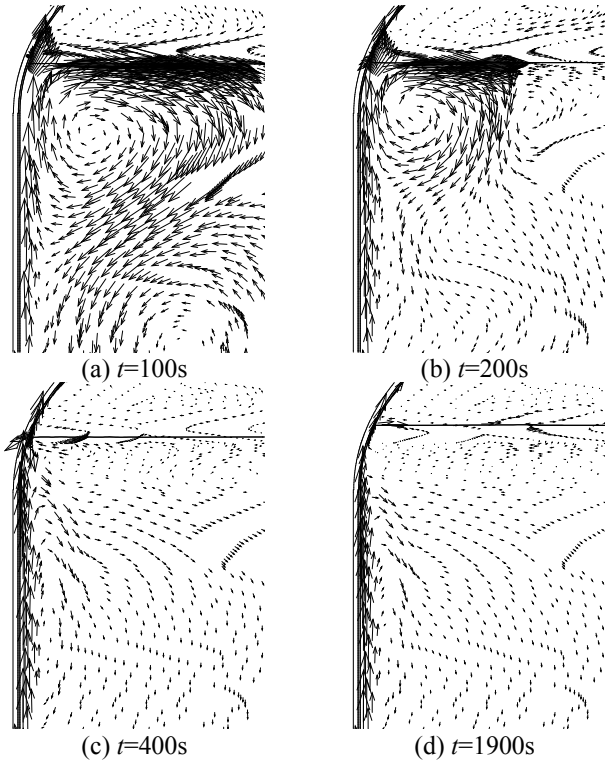

Fig. 11 Velocity vectors of the LH2 test tank

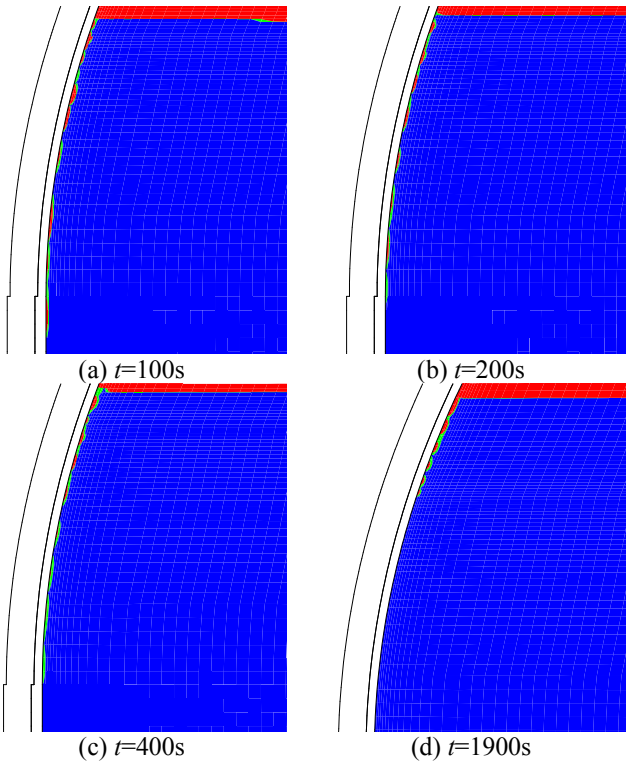

Fig. 12 Phase contours of the LH2 test tank

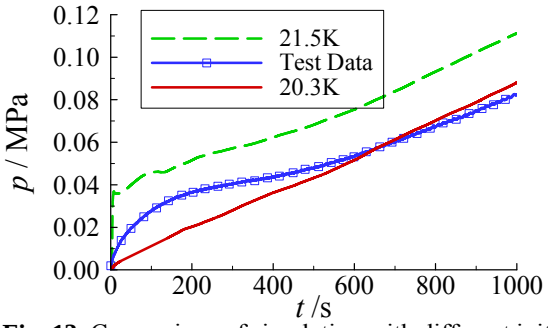

Fig. 13 Comparison of simulation with different initial temperatures (T_0=21.5K and T_0=20.3K) and test result of pressure in the liquid hydrogen test tank

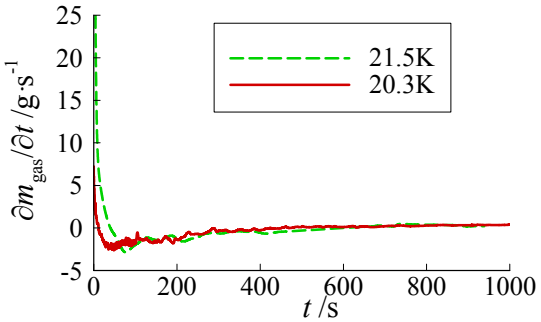

Fig. 14 Comparison of simulation results of evaporation rate with different initial temperatures (T_0=21.5K and T_0=20.3K)

Therefore, the deflection in the unstable stage as shown in Fig. 6 is imputed to the practical non-uniform initial temperature distribution and local overheating in cryogenic liquid. Since the liquid become saturated after the pressure leap, the pressure rise rates of the two simulations in their quasi-steady periods is quite close. Similarly, the cause of the initial transient period shown in Fig. 3 is caused by the overheat reflected by Fig. 4.

CONCLUSION

Comparisons between simulation results and tests validate the VOF model with a compressible gas phase and a phase change model built on the assumption of thermodynamic equilibrium. The simulated pressure and temperature variation are both very close to the test data of a liquid hydrogen self-pressurization test implemented by NASA. The deviation is much smaller than other existing simulation researches. The other comparison is made with a liquid hydrogen self-pressurization test conducted by a Chinese research institute. The difference of 6.1% between the simulation quasi-steady pressure rise rate and the test data proves the reliance of this CFD model.

It is revealed that the thermal stratification in the liquid hydrogen tank is affected by both the propellant flow and the heating from the wall and the gas. And the temperature distribution change weakens the convection. The deflection in the unstable stage of the second simulation is imputed to the initial overheat of the liquid hydrogen. The initial overheat causes sharp evaporation and significantly affects the transient stage of tank pressure rise. But small difference of initial temperatures has less influence on quasi-steady pressure rise rate.

REFERENCES

[1]. Van Dresar, N.T., C.S. Lin and M.M. Hasan, Self-Pressurization of a Flightweight Liquid Hydrogen Tank: Effects of Fill Level at Low Wall Heat Flux. 1992, 30th Aerospace Sciences Meeting and Exhibit: Reno.

[2]. Barsi, S. and M. Kassemi, Numerical and Experimental Comparisons of the Self-Pressurization Behavior of an LH2 Tank in Normal Gravity. Cryogenics, 2008. 48: p. 122-129.

[3]. Hasan, M.M., C.S. Lin and N.T. Van Dresar, Self-Pressurization of a Flightweight Liquid Hydrogen Storage Tank Subjected to Low Heat Flux. 1991, 1991 ASME/AIChE National Heat Transfer Conference: Minneapolis.

[4]. Estey, P.N., D.H. Lewis Jr. and M. Connor, Prediction of a Propellant Tank Pressure History Using State Space Methods. J. Spacecraft and Rockets, 1983. 20(1): p. 49-54.

[5]. Schallhorn, P. and L. Grob, Upper Stage Tank Thermodynamic Modeling Using SINDA/FLUINT. 2006, 42nd AIAA/ASME/SAE/ASEE Joint Propulsion Conference & Exhibit: Sacramento.

[6]. Barsi, S. and M. Kassemi, Validation of Tank Self-Pressurization Models in Normal Gravity. 2007, 45th AIAA Aerospace Sciences Meeting and Exhibit: Reno.

[7]. Mattick, S.J., et al., Progress in Modeling Pressurization in Propellant Tanks. 2010, 46th AIAA/ASME/SAE/ASEE Joint Propulsion Conference & Exhibit: Nashville.

[8]. Mukka, S. and M. Rahman, Computation of Fluid Circulation in a Cryogenic Storage Vessel. 2004, 2nd International Energy Conversion Engineering Conference: Providence.

[9]. Kittel, P. and D.W. Plachta, Propellant preservation for mars missions. Adv. Cryogenic Engng, 2000. 45: p. 443.

[10]. Xu, J., Boiling heat transfer and gas-liquid two-phase flow. 2001, Beijing: Atomic Energy Press.

[11]. Nguyen, H., Zero-g thermodynamic venting system (TVS) performance prediction program, in NASA-CR-193982. 1994, Rockwell International Corp.: Downey.

[12]. Zilliac, G. and M.A. Karabeyoglu, Modeling of Propellant Tank Pressurization. 2005, American Institute of Aeronautics and Astronautics: Tucson, Az.